# Electronic structure of $CrBr_3$ studied by x-ray photoelectron spectroscopy

I. Pollini
*Istituto Nazionale di Fisica per la Materia (INFM), Dipartimento di Fisica-Università degli Studi di Milano, Via Celoria, 16-20133 Milano, Italy*

(Received 17 June 1999; revised manuscript received 27 July 1999)

The electronic structure of high-spin $CrBr_3$ has been investigated by using x-ray photoelectron and electron energy-loss spectroscopy. Valence-band and Cr2*p* core-level spectra have revealed satellite structures on the high-binding energy side of the main emission line around 7.7 and 11 eV, respectively. The weak satellite structure observed in the valence-band spectrum can be explained by a charge transfer mechanism, if the *p-d* hybridization is sufficiently large. Nevertheless, for the interpretation of the Cr2*p* satellite structure ($\cong$11 eV), competition between the charge transfer and the exciton models needs to be considered.
[S0163-1829(99)12247-1]

## I. INTRODUCTION

Chromium tribromide ($CrBr_3$), a ferromagnetic material with an energy gap of about 2.1 eV, is a promising material for optical isolators, magnetic sensors, and rewritable optical memories.[1,2] In recent years, there has been an increasing demand for materials with high magneto-optical effects, such as Kerr rotation and magnetic-circular dichroism.[3–5] Magnetic studies on the 7.20-eV interband ($4p \rightarrow 4s,4p$) exciton around the Curie temperature has been also made some time ago.[6,7] A study of the electronic structure in $CrBr_3$ is thus important not only for a fundamental understanding of the material, but also for technological applications. Unfortunately, the transition-metal compounds (TMC), like $CrX_3$ ($X=$Cl, Br) or $Cr_2O_3$, are more complicated than ordinary semiconductors or insulators (i.e., alkali halides), in that they contain both bandlike and localized *d* states.[8] Moreover, it is well known that the *d*-electron correlation is an essential concept for the actual band structure of these *narrow d*-band materials and that their *d-d* or *p-d* gaps originate from the *d*-electron localization, as explained in the Mott-Hubbard (MH) or Zaanen-Sawatzky-Allen (ZSA) models.[9,10] X-ray photoemission (XPS) is a powerful method to investigate the electronic structure of TMC's and the photoelectron energy distribution curves for the valence region are directly related to the calculated density of states in the valence band. Also, much of the understanding of the electronic structure of late 3*d* TMC's comes from the study of the core-level (*c*-XPS) and valence-level (VB-XPS) x-ray photoelectron spectroscopy satellites. In *c*-XPS the Coulomb attraction between the core hole and the localized valence electrons and the resulting screening response have to be taken into account in order in interpret the photoemission (PE) spectra adequately. There are currently two models in the literature to describe satellite structures in PE spectra of TMC's: the charge transfer[11,12] (CT) and the exciton models.[13] The CT model is equivalent to a molecular-orbital picture, where a TM *d* level mixes with a ligand *p* level and in the ground state the bonding orbital is filled and the anti-bonding is empty. The *screening* of the core hole lowers the *d* level energy with respect to the energy of the ligand *p* levels, so that the bonding and anti-bonding orbitals change, resulting in a nonvanishing probability for each final state to be occupied. The physics is described in terms of a few parameters, namely the on-site *d-d* Coulomb repulsion energy *U*, the charge transfer (CT) energy $\Delta$, the Coulomb attraction energy *Q* between the core hole and 3*d* electrons, and the ligand *p*-metal *d* hybridization energy *T*, which show systematic trends with formal valence state and atomic number across the 3*d* transition-metal series.[14–16] Within the framework of *cluster model* (CM), the XPS core satellites can also be used to study the valence electronic structures indirectly, as in the case of CuO and Cu halides.[17] One problem associated with the CT interpretation of the satellite structures of the *early* TMC's is the ambiguity of their origin. In the exciton model of de Boer, Haas, and Sawatzky.[13] the polarization of the ligands is responsible for *screening* the core hole at the TM site, and satellites arise due to the electron-hole pairs on the ligands. Another possibility is that the satellites are due to electron energy-loss (EEL) processes within the crystal bulk. Inelastic loss peaks in the EEL spectra, located at energies close to those of the satellite structures in the PE spectra, might imply that weak structures result from the energy-loss processes. However, the situation does not seem quite satisfactory for the $Cr_2O_3$ (Refs. 18 and 19) and $CrX_3$ insulators,[20,21] where a simple-ligand field (LF) picture has been used to describe the VB-XPS data. In $CrBr_3$ and $CrCl_3$ compounds, the parameter values of $\Delta$ (5.5–6.5 eV), *U* (3.0–3.5 eV), and *T* ($\sim$1.5 eV) seem to indicate the presence of weak-electron correlations and intermediate hybridization effects and the parameter estimates are close to the values reported in 2*p*-XPS for $MnCl_2$ ($\Delta=4.5$ eV, $U=3.2$ eV, and $T=1.5$ eV) and $MnBr_2$.[22] Since a comprehensive study of $CrBr_3$ has not been performed so far, here we report PE spectra of $CrBr_3$ compounds together with a new VB-XPS of $CrCl_3$ measured on freshly grown samples. Also, in order to understand the nature of the high-energy structures appearing in the PE spectra, EEL measurements have been made. The discussion of the valence band and 2*p*-XPS photoelectron structures in $CrBr_3$ will be made by considering both the configuration interaction cluster model and the exciton model approximations in order to get additional knowledge on the intricate electronic properties of Cr halides. The *satellite* features observed in the spectra of the Cr $3d^3$ system could in principle

 

affect the classification of $CrX_3$ materials, according to the ZSA theory. The examples of $Cr_2O_3$ and $Ti_2O_3$ are interesting in this regard: for example, $Cr_2O_3$, a traditional MH insulator[9,10,23] has been recently reclassified by means of a CM analysis as an intermediate material, owing to its large hybridization energy.[15,16]

## II. EXPERIMENT

High stoichiometric and rather pure crystals have been prepared from the vapor phase with a flow-system method at about 750 °C. The identity of $CrBr_3$ crystals was established by means of high-energy electron Bragg diffraction patterns and chemical analysis, as it was earlier made in $CrCl_3$.[20] The low-temperature structure of $CrBr_3$ ($T<450$ K) is the same of the layer structure $BiI_3$ (space group $C_{3i}$). Crystalline samples of $CrBr_3$ and $CrCl_3$ were used in the experiments in order to minimize possible surface effects. Crystals were cleaved *in situ*, at pressures of the order of $10^{-10}$ mm, Hg in order to get fresh surfaces and to clean them from the presence of carbon and oxygen impurities. The impurity content was checked by XPS measurements: in no samples could one find any trace of impurity except for the unavoidable carbon and oxygen signals. Before measurements the *cleaved* $CrX_3$ crystals were subjected to $Ar^+$-ion bombardment to clean them up from the presence of both the C 1*s* (~280 eV) and O 1*s* peaks (~535 eV), which may arise from adsorbed water and carbon oxides. While the O 1*s* peak was easily eliminated in the spectra of both samples, a fairly strong O 1*s* peak persisted in the spectrum of $CrBr_3$. This required a subsequent cleaning by a sputtering-annealing cycle until very few or no traces of impurities were detected by XPS spectroscopy. However, it was noted that the satellite energy distance $E_S$ from the main peaks was not significantly affected by the presence of some residual impurities in the VB-XPS and Cr 2*p*-XPS measurements.

The experiments were performed with a XPS spectrometer ESCALAB MKII manufactured by the Vacuum Generators, equipped with a monochromatized $AlK_{\alpha 1,2}$ (1486.6 eV) radiation. Photoelectrons were analyzed along the normal of the sample with an energy resolution of about 1.0 eV. Charging of the samples during the photoemission experiment was monitored by heating some of the samples to 100–120 °C. A small amount of steady-state charging was present during measurements: the charging effect however did not distort spectra, as was verified by repeating measurements, although it did prevent a precise determination of the Fermi level ($E_F$). However, this will not affect our discussion because we will only focus on the relative positions of photoemission peaks. The electron energy-loss (EEL) spectrum of $CrBr_3$ crystals was obtained by means of an electronic spectrometer, where the monoenergetic electron beam (50 keV) was transmitted through the specimen and scattered by an angle of 1 mrad. The energy analysis was performed by a cylindrical electrostatic sector with an angle of deflection of $\pi/2\sqrt{2}$. The spectral resolution, defined as the half width of the elastic peak, is better of 0.5 eV. The apparatus geometry ensures that the momentum transfer and the electric vector lie in the basal plane of $CrBr_3$ crystals ($\mathbf{E}\perp\mathbf{c}$).[24] The EEL spectra allow to get an estimate of the energy of the charge transfer transitions (related to the $\Delta$ parameter) and interband transitions (probably related to the Cr core-level satellite energy) with a different experimental technique. The energy values measured in EELS have been found in agreement with the values obtained in the reflectance spectra of $CrBr_3$.[21]

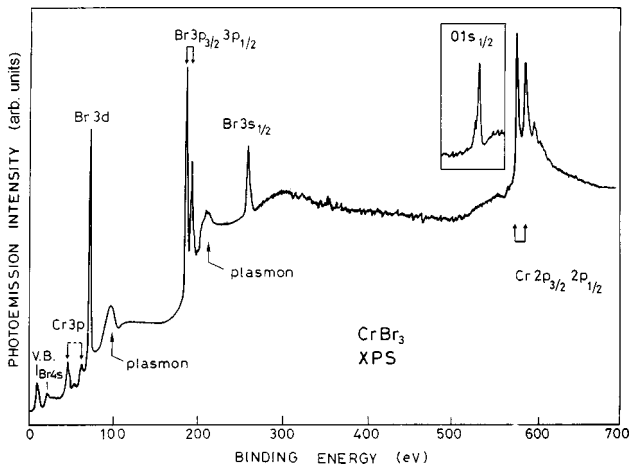


FIG. 1. X-ray photoelectron survey spectrum of a cleaned $CrBr_3$ crystalline sample after its cleaving *in situ*. In the insert it is instead shown the presence of the O 1*s* line as observed after the ion bombardment of freshly grown crystals. The Al $K\alpha_{12}$ radiation (1486.6 eV) source was used during the experiment.

## III. RESULTS AND DISCUSSION

Figure 1 shows the survey spectrum of *cleaved* and cleaned $CrBr_3$ crystals after some $Ar^+$-ion bombardment at room temperature. The location and identities of the observed spectral features are reported versus the binding energy up to 700 eV: chromium ($Cr3p_{1/2}$, $Cr3p_{3/2}$, $Cr2p_{1/2}$, and $Cr2p_{3/2}$) and bromine ($Br3d$, $Br3p_{1/2}$, $Br3p_{3/2}$) peaks are indicated in the figure. In the insert, one can note the presence of a residual, fairly strong oxygen ($O1s$) line observed at about 537 eV, after cleaving the sample in ultravacuum, but before the cyclic sputtering-annealing process required for a careful cleaning.

Figures 2(a) and 2(b) report VB spectra of $CrCl_3$ and $CrBr_3$, shown together with the spectrum of $Cr_2O_3$ (Ref. 16) for comparison [Fig. 2(c)]. The spectra are rather similar and can be divided into the main band (1–10 eV) and the satellite region (10–15 eV). In $CrX_3$, the main $Cr3d$ structure, partly mixed with the nearby $Cl3p$ and $Br4p$ bands, is located around 3 eV and was earlier assigned to $Cr3d^2$ (poorly screened) final states.[21] The final-state peak position for a BIS experiment has been also indicated in Figs. 2(a) and 2(b), its position being extrapolated from the ultraviolet reflectance and EEL spectra of $CrCl_3$ and $CrBr_3$. The PES and BIS peaks in Cr halides give an indication of the $Cr3d^2$ and $Cr3d^4$ energy-level positions, whose separation yields the Coulomb energy $U$ to zero order in $CrBr_3$ and $CrCl_3$ ($U\simeq 3.6$ and 4.6 eV). Energy corrections due to *p-d* hybridization will then reduce the solid-state value $U$ and the ''bare'' value of $U$ (of atomic origin) can be estimated anew, if one is able to take into account the hybridization shifts $\delta's$ in Cr halides. In $Cr_2O_3$, the satellite feature ($S$) has an energy separation ($E_S$) from the main line given by $E_S\cong 11.5$ eV, while in $CrCl_3$ and $CrBr_3$ the weak satellite structures have a dis-

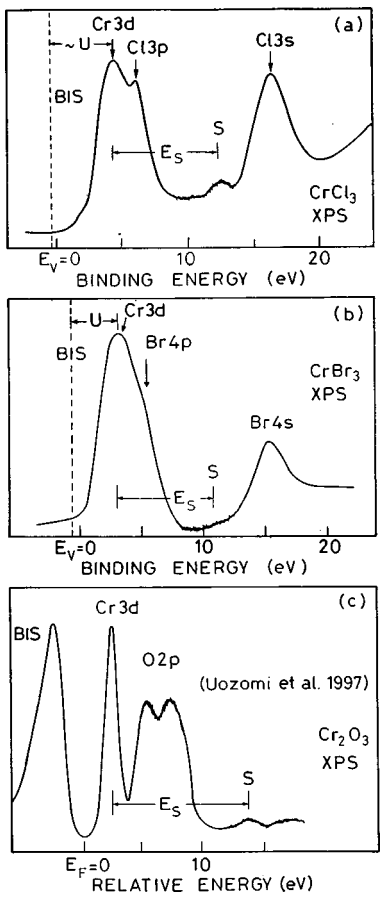


FIG. 2. X-ray photoelectron spectra in the valence-band region of $CrBr_3$, $CrCl_3$, and $Cr_2O_3$ (Uozomi *et al.*, Ref. 16).

tance $E_S \cong 7.9$ and 7.7 eV, respectively.

Figure 3 reports the characteristic electron energy-loss structures *A*, *B*, *C*, and *P* measured in $CrBr_3$ at room temperature. Structures *A* and *B* observed around 4 and 6 eV are assigned to charge-transfer transitions from the Br4*p* to the Cr3*d* orbitals.[7,21] The inelastic peak *C* observed at $\cong$10.5 eV in both EEL and reflectance spectra is instead assigned to Br4$p \rightarrow$Cr4*s* interband transitions: one can note that its excitation energy is rather close to the energy $E_S \cong 11$ eV of the satellite in the Cr2*p*-XPS, so that the attribution of this satellite to an interband transition within the scheme of the exciton model seems reasonable.

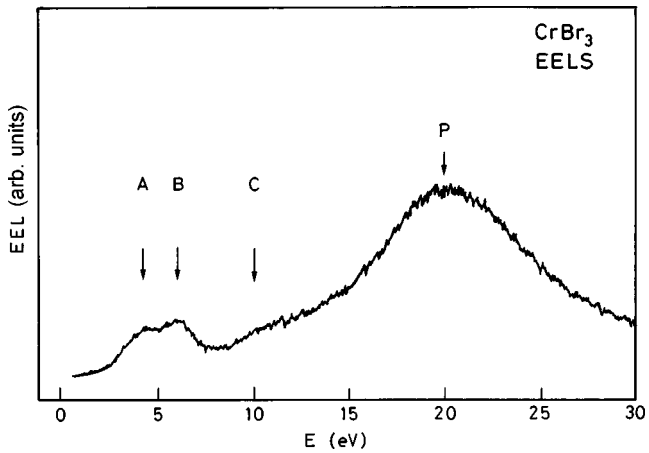


FIG. 3. Characteristic electron energy-loss spectrum of $CrBr_3$ crystals measured at room temperature.

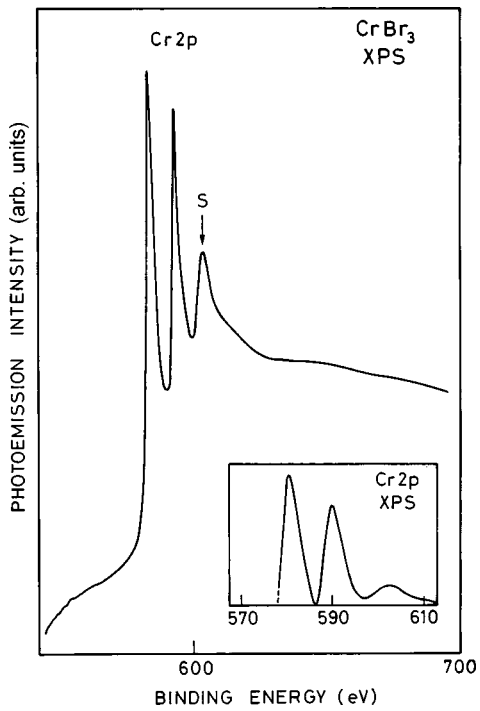


FIG. 4. X-ray photoelectron spectra of $CrBr_3$ and $Cr_2O_3$ in the Cr 2*p* region.

Figure 4 shows the satellite feature observed in the 2*p*-XPS of $CrBr_3$: the $2p_{3/2}$ (581 eV) and $2p_{1/2}$ (592 eV) main lines originate from the spin-orbit split core state and the satellite *S* is observed at $E_S \cong 603$ eV (in the insert). Both in $Cr_2O_3$ and $CrBr_3$ only the satellite associated with the main $2p_{1/2}$ peak is observed, while the one associated with the $2p_{3/2}$ peak is overlapped with the $2p_{1/2}$ main peak and not seen: in $Cr_2O_3$, $E_S = 11.5$ eV and in $CrBr_3$, $E_S \cong 11$ eV. We remark that the satellite energy distance in $CrBr_3$ is lower than the value of $E_S = 13.2$ eV reported in Okusawa's paper.[25] A possible explanation for the satellite origin in the 2*p*-XPS is that of a *charge transfer* from the ligand *p* (i.e., Br4*p*) to the metal 3*d* electrons (Cr3*d*) in presence of a large *p-d* hybridization, as it is generally proposed for many first-row TMC's. However, in Cr2*p*-XPS the satellite distance $E_S$ seems somewhat larger than expected from optical gaps and molecular calculations. According to some authors.[26,27] the observed satellite can also reflect a transfer from the outer ligand *p* to metal 4*s*,4*p* orbitals: an argument for this is that in optical spectra, peaks at about the same energy appear, which are assigned to the same kind of transitions. If one compares the satellite structure in $CrCl_3$ and $CrBr_3$ with the data from the vacuum-ultraviolet spectra one finds a region up to 6–7 eV, which is ascribed to CT transitions from Cl3*p* and Br4*p* orbitals to Cr3*d* orbitals. The reflectance peaks around 8.6 eV in $CrCl_3$ and 7.2 eV in $CrBr_3$ are assigned to excitonic transitions from the anion *p* to TM conduction-band orbitals. For the Cr halides, unfortunately, the reported data are not conclusive since for Cr3*p* the energy distances are found over 20 eV above the main line,[25] but for Cr2*p* different values are reported: i.e., 10.3 eV in $CrCl_3$ and 11 eV in $CrBr_3$.[28] It seems as though, de-

TABLE I. Solid state parameters (eV) of early transition metal compounds estimated from valence-band and $2p$-XPS core-level spectra, UV reflectance and EEL data.

| Compound | $d^n$ | $\Delta$ | $U$ | $T$ | $T_{\text{eff}}$ | $E_s$ | $Q$ | Reference |
|---|---|---|---|---|---|---|---|---|
| $Ti_2O_3$ | $d^1$ | 6.0 | 4.5 | 3.0 | 6.9 | 12 | 5.3 | 15;16 |
| $Cr_2O_3$ | $d^3$ | 5.2 | 5.2 | 3.5 | 7.6 | 11.5 | 6.5 | 15;16 |
| $CrCl_3$ | $d^3$ | 6.5 | 3.5;3.3 | 1.7 | 3.6 | 7.9 | 4.7 | |
| $CrBr_3$ | $d^3$ | 5.5 | 3.0;3.1 | 1.7 | 3.6 | 7.7 | 4.3 | |
| $MnF_2$ | $d^5$ | 9.0 | 3.2 | 1.5 | 4.25 | 6.4 | 4.5 | 22 |
| $MnCl_2$ | $d^5$ | 4.5 | 3.2 | 1.5 | | 5.4 | 4.5 | 22 |
| $MnBr_2$ | $d^5$ | 3.2 | 3.2 | 1.4 | | 5.2 | 4.5 | 22 |

pending on the ligands or cations, there may be different mechanisms that give rise to satellite structures. In this context it is likely that the exciton satellite mechanism might be active in early TMC's specially when $\Delta$ is large and $Q$ is small and there are many empty $3d$ orbitals. Thus the satellite structures observed at binding energies of 7.7–7.9 eV in the VB-XPS of Cr halides could actually assigned to interband *excitons* connected to ligand $p$ to metal $4s$,$4p$ interband transitions as in optical spectra.

Alternatively, one can discuss the VB-XPS data in $CrBr_3$ (and $CrCl_3$) and the origin of the satellites at 7.7–7.9 eV in the framework of the CT model,[12] by considering that a sufficiently large $p$-$d$ hybridization may shift the 6–7 eV *charge-transfer* transitions to higher energy, as observed in the photoemission spectra of many early TMC's.[29] In this case, the effective hybridization energy $T_{\text{eff}}$ between the $3d^2$ and $3d^3L^1$ photoemission final states can be estimated within the model limits by

$$T_{\text{eff}}=[(6-n)(T_{t2g})^2+4(T_{eg})^2]^{1/2} \quad (n\leqslant 3), \tag{1}$$

where $T_{t2g}$ and $T_{eg}$ are the one-electron mixing matrix elements $T_{eg}=\langle e_g|H|Le_g\rangle=T$ and $Tt_{2g}=\langle t_{2g}|H|Lt_{2g}\rangle=0.5\,\text{T}$, and the full Hamiltonian is described in references 15 and 16. When the Hamiltonian is restricted to $d^n$ and $d^{n+1}L^1$ configurations, the main peak-satellite splitting $E_S$ in the valence-band spectra is given by

$$E_S=[(\Delta-U)^2+(4T_{\text{eff}})^2]^{1/2}. \tag{2}$$

In the limit of $|\Delta-U|\ll 2T_{\text{eff}}$, the value of $E_S$ can be approximated by $2T_{\text{eff}}$. In many early TMC's, the parameters $\Delta$ and $U$ have comparable values and the electronic structure is mainly determined by the effective hybridisation $T_{\text{eff}}$. Analogous to the discussion on $2p$-XPS in early TMC's, the main $3d$ features and the $S$ structure are separated by $E_S$ because of the $p$-$d$ hybridization with a separation given by Eq. (2), where the valence-band parameter $U_{dd}$ is substituted to $U_{dc}$ (indicated also with $Q$), valid for core-level spectroscopy.[15,16,22] In $CrBr_3$ one gets: $|\Delta-U_{dd}|\cong 2.5\,\text{eV}$, since $\Delta=5.5\,\text{eV}$ and $U_{dd}=3.0\,\text{eV}$, while $E_S\approx 2T_{\text{eff}}=7.7\,\text{eV}$, and from Eq. (2) one obtains the parameters values reported in Table I. In the Cr$3d$-XPS spectra of Figs. 2(a) and 2(b), the main emission Cr $3d$ structure corresponds to *mixed* $3d^2$ (mainly) and $3d^3L^1$ final state configurations and the satellite $S$ to $3d^3L^1$ (mainly) and $3d^2$ ($3d^4L^2$) configurations, because of the effective hybridization. In $2p$-XPS of $CrBr_3$ crystals, a value of $E_S\cong 11\,\text{eV}$ has been here found, while values of $E_S\cong 10.3$ and 11.0 eV for $CrCl_3$ and $CrBr_3$, respectively, have been reported earlier.[28] In Table I, theoretical and experimental CM parameters for $CrBr_3$ and $CrCl_3$ and some early TM oxides have been reported. We can see that $Ti_2O_3$ seems to be a MH insulator, while $Cr_2O_3$ is probably an intermediate compound and the $MnX_2$ ($X=\text{Cl, Br}$) dihalides are ''marginal'' CT compounds. $CrX_3$ materials seem similar to $Ti_2O_3$ and $MnF_2$ compounds and are considered MH insulators. We note also that the values of $T$ obtained in the ''ionic'' $CrBr_3$ and $CrCl_3$ compounds in the present work are in fine agreement with the value of $T\sim 1.5\,\text{eV}$ previously estimated.[21]

Photoconductivity spectra of $CrBr_3$ crystals have been reported:[30] These data give an indication of its conductivity energy gap $E_g=2.1\,\text{eV}$. If the forbidden gap is of $d$-$d$ character,[9,10,21] it involves holes and electrons in the $3d^{n-1}$ and $3d^{n+1}$ Hubbard bands, somewhat broadened and shifted in energy by the effective hybridization in the solids. Below 2.5 eV weak photocurrent features are observed with an intensity lower by a $\sim 10^2$ factor than the photoconductivity edge extending to about 3 eV, where starts the onset of the charge transfer excitons observed in reflectance and EEL spectra. We can now get an estimate of the hybridization shift parameter $\delta$ and try to get a better determination of the correlation energy $U$ in $CrX_3$ materials. According to the ZSA theory, the energy gap $E_g$ in a MH insulator ($\Delta>U$) is

$$E_g=U+\delta-w, \tag{3}$$

where $w$ is the dispersional $3d$ bandwidth. We take as value of bandwidth $w$ that measured from the UPS and BIS spectra, that is $w\cong 1.0\,\text{eV}$.[16,31] With the values of $U_{\text{solid}}=3.6\,\text{eV}$, $E_g=2.1$ and $w\cong 1\,\text{eV}$, one gets a lower limit for $\delta=0.5\,\text{eV}$ from Eq. (3). From the zero-order value of $U=3.6\,\text{eV}$ in Fig. 2, one can estimate the correlation energy $U_{\text{bare}}$ ($=U_{\text{solid}}-\delta$)$=3.1\,\text{eV}$ for $CrBr_3$, listed in Table I together with that of $CrCl_3$ obtained in the same manner.[32] The $U$ value is reduced in $CrX_3$, since the states near the energy gap are in part affected by the hybridization energy (note in Fig. 2 that the Cr $3d$ levels are partly mixed with the underlying valence ligand $p$ states). Also, it is worth noting that the present estimate of the (atomic) $U$ parameter (3.1 eV) is in agreement with the value ($U\cong 3.0\,\text{eV}$) obtained in the spectroscopic approach and, besides, that this value of $U$ in $CrBr_3$ is closer to that determined for $CrCl_3$ ($U=3.3\,\text{eV}$), as it should be, since the $U$ parameter represents an atomic property. Thus, the analysis of the valence band XPS results

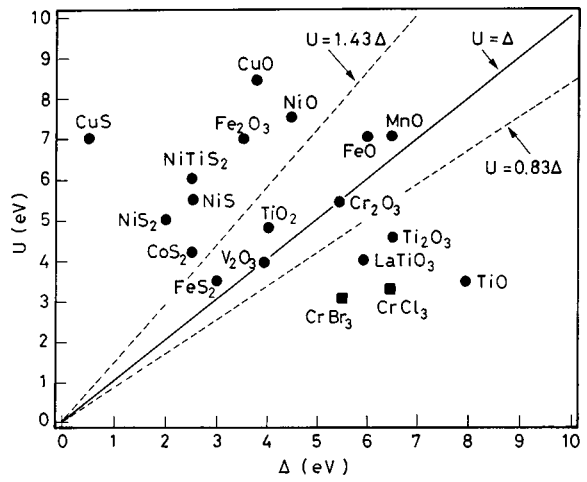


FIG. 5. Δ-*U* diagram across the transition-metal series from Ti to Cu (Ref. 14). The region above the $\Delta = U$ line is the charge transfer regime, while that below is the Mott-Hubbard regime. Compounds falling close the $\Delta = U$ line are intermediate between the two regimes (dark circles). The chromium trihalides are indicated by dark squares.

seems to indicate that the CM is able to describe the satellite properties in Cr halides, as in the case of many early TMC's, and that, in addition, quite reasonable parameters are obtained, in line with the typical parameters reported for early TM compounds. The present results seem to indicate that the covalency between the metal *d* states and the ligand *p* states makes the distinction between CT an MH compounds less clear for some early TMC's, which may fall in the intermediate region of the Δ-*U* diagram (see Fig. 5). For example, $Fe_2O_8$ is predicted to be a CT insulator (as NiO and CuO), while $Cr_2O_8$ is considered close to the borderline, since the Δ, *U* and *T* values are of comparable values. Also $CrCl_3$ and $CrBr_3$ compounds might fall into the *intermediate* region of the Δ-*U* plot, but the ''ionic'' Cr trihalides are still *inside* the MH region because of the large value of the charge transfer energy Δ and, besides, they are located in the plot close to Mott-Hubbard insulators, such as TiO and $Ti_2O_3$.[15,16] Moreover, the Δ-*U* diagram seems to indicate that only a few compounds are left in the lower right region of the plot, after that some recent works in the literature have shifted many traditional MH insulators into the intermediate region.

## IV. CONCLUSION

In summary, the presence of satellites in the valence band and $2p$ core-level photoemission in $CrCl_3$ and $CrBr_3$ suggests to reconsider the simple LF interpretation earlier proposed for these compounds. The presence of a sufficiently large *p-d* hybridization in the final states seems to reduce somewhat the ionic character of Cr trihalides, with a consequent electron redistribution, which can in part affect its electronic structure and band-gap character. The main peak configuration could have been written as $d^3L^1$, as in late TMC's, but the gap character changes from a $(d^3L^1$-$d^4)$-type (CT regime) to the $(d^2$-$d^4)$-type (MH regime) because of the relatively strong ionicity (large Δ) of the compounds. This in line with the change of the gap character in some early TMC's (e.g., TiO and $Ti_2O_3$) and would then correspond to the inversion of the $3d^nL^1$ and $3d^{n-1}$ states in the $(N$-$1)$-UPS scheme of levels shown in Ref. 10. Thus, since it is *mainly* the splitting of the $3d$ bands, which makes $CrX_3$ insulating and determines their electrical nature, Cr trihalides are rightly described as typical *Mott insulators*.


[1] M. Abe and M. Gomi, J. Magn. Magn. Mater. **84**, 222 (1990).
[2] J. F. Jr Dillon, J. Magn. Magn. Mater. **84**, 213 (1990).
[3] W. Jung, J. Appl. Phys. **36**, 2422 (1965).
[4] J. F. Dillon, H. Kamimura, and J. P. Remeika, Phys. Chem. Solids **27**, 1531 (1966).
[5] G. Pedroli, I. Pollini, and G. Spinolo, J. Phys. C **8**, 2317 (1975).
[6] L. Nosenzo, E. Reguzzoni, G. Samoggia, G. Guizzetti, and I. Pollini, Solid State Commun. **29**, 793 (1979).
[7] L. Nosenzo, G. Samoggia, and I. Pollini, Phys. Rev. B **29**, 3707 (1984).
[8] S. Antoci and L. Mihich, Phys. Rev. B **18**, 5768 (1978).
[9] N. F. Mott, *Metal-Insulator Transitions*, 2nd ed. (Taylor & Francis, London 1990), and references therein.
[10] J. Zaanen, G. A. Sawatzky, and J. W. Allen, Phys. Rev. Lett. **55**, 418 (1985).
[11] A. Fujimori and F. Minami, Phys. Rev. B **30**, 957 (1984).
[12] K. Okada and A. Kotani, J. Phys. Soc. Jpn. **61**, 4619 (1992).
[13] D. K. G. de Boer, C. Haas, and G. A. Sawatzky, Phys. Rev. B **29**, 4401 (1984).
[14] A. E. Bocquet, T. Mizokawa, T. Saitoh, H. Namatame, and A. Fujimori, Phys. Rev. B **46**, 3771 (1992).
[15] A. E. Bocquet, T. Mikozawa, K. Morikawa, A. Fujimori, S. R. Barman, K. Maiti, D. D. Sarma, Y. Tokura, and M. Onoda, Phys. Rev. B **53**, 1161 (1996).
[16] T. Uozomi, K. Okada, A. Kotani, R. Zimmerman, P. Steiner, S. Hüfner, Y. Tezuka, and S. Shin, J. Electron Spectrosc. Relat. Phenom. **83**, 9 (1997).
[17] G. van der Laan, C. Westra, C. Haas, and G. A. Sawatzky, Phys. Rev. B **23**, 4369 (1981).
[18] G. K. Wertheim, H. G. Guggenheim, and S. Hufner, Phys. Rev. Lett. **30**, 1050 (1973).
[19] D. E. Eastman and J. L. Freeouf, Phys. Rev. Lett. **34**, 395 (1975).
[20] I. Pollini, Phys. Rev. B **50**, 2095 (1994).
[21] I. Pollini, Solid State Commun. **106**, 549 (1998).
[22] J. Park, S. Ryu, M. Han, and S. J. Oh, Phys. Rev. B **37**, 10 867 (1988).
[23] X. Li, L. Liu and V. E. Henrich, Solid State Commun. **12**, 1103 (1992); K. E. Smith and V. E. Henrich, *ibid.* **68**, 29 (1998).
[24] B. Carricaburu, J. Ferré and P. Perrier, J. Microsc. Spectr. Electron **2**, 39 (1977).
[25] M. Okusawa, Phys. Status Solidi B **124**, 673 (1984); M. Okusawa, K. Tsutsumi, T. Ishii, and T. Sagawa, J. Phys. Soc. Jpn. **51**, 510 (1982).
[26] I. Ikemoto, K. Ishii, H. Kuroda, and J. M. Thomas, Chem. Phys. Lett. **28**, 55 (1974).
[27] A. Gupta and J. A. Tossel, J. Electron Spectrosc. Relat. Phenom. **26**, 223 (1982).
[28] G. A. Vernon, G. Stucky, and T. A. Carlson, Inorg. Chem. **15**,

278 (1976). All compounds were prepared without further purifications: it is remarkable that the observed satellite distances from the main lines in $CrCl_3$ and $CrBr_3$ obtained by these authors have the same values as in the *cleaved* and *cleaned* samples of the present work (10.3 and 11 eV, respectively).

[29] J. C. Parlebas J. Phys. I **2**, 1369 (1992).

[30] K. K. Kanazawa and G. B. Street, Phys. Status Solidi **38**, 445 (1970).

[31] T. Uozomi, K. Okada, and A. Kotani, J. Phys. Soc. Jpn. **62**, 2595 (1993).

[32] In $CrCl_3$, with the values of $U_{solid}=4.6$ eV. $E_g=2.3$ eV and $w \cong 1$ eV, one gets a lower limit for $\delta=1.3$ eV from Eq. (3): from the zero-order value of $U=4.6$ eV, one can estimate the correlation energy $U_{bare}(=U_{solid}-\delta)=3.3$ eV.